MEDWIN PUBLISHERS
Committed to Create Value for Researchers

Nanomedicine & Nanotechnology Open Access
ISSN: 2574-187X

Flame Synthesis of Nanocrystalline Yttria Stabilized Zirconia Powders from Aqueous Precursors

Ganguly R[1,2]*, Mandal S[1], Rao S[1] and Bhattacharya SS[2]

[1]Carborundum Universal Limited, Industrial Ceramics Division, India
[2]Department of Metallurgical and Materials Engineering, IIT Madras, India

***Corresponding author:** Ritendu Ganguly, Carborundum Universal Limited, Industrial Ceramics Division, Hosur–635126, Tamil Nadu, India, Email: gangulyr@cumi.murugappa.com

Research Article
Volume 5 Issue 3
Received Date: November 12, 2020
Published Date: December 08, 2020
DOI: 10.23880/nnoa-16000205

Abstract

Flame reactors are considered to be one of the promising and versatile equipment for making nanocrystalline ceramic powders. Flame synthesis of nanocrystalline yttria stabilized zirconia (YSZ) was carried out using zirconium oxy-nitrate and yttrium nitrate as precursors. The yttria (Y2O3) content was systematically varied from 8 mol% to 12 mol.% in zirconia in order to stabilize either partially or fully the monoclinic crystal structure. Precursor solutions of 1(M) concentration were prepared by dissolving in de-ionised water. X-ray diffraction of the as-synthesized powders confirmed that the cubic phase had been stabilized, except in the case of 8 mol% YSZ prepared from the precursor solution. All the powders were nanocrystalline in nature with the crystallite size increasing from 45 nm to 62 nm with increasing yttria content. Scanning electron microscopy revealed the powder characteristics to be typical of an aerosol based processing technique. The specific surface area, measured by nitrogen adsorption, was 14-15 m^2g^{-1}. By pressureless sintering technique, more than 99% of the theoretical density was achieved.

Abbreviations: YSZ: Yttria Stabilized Zirconia; SOFC: Solid Oxide Fuel Cell; XRD: X-Ray Diffraction; BET: Brunauer-Emmett-Teller.

Introduction

Yttria stabilized zirconia (YSZ) exhibits good oxygen ion conductivity at elevated temperature which makes it useful for use in various applications such as anesthesia monitors, respirators and oxygen concentrators etc. for medical usage. Currently YSZ ceramic is being employed as oxygen separation membrane [1] for producing oxygen enriched air which is required for medical applications [2] and also for producing oxygen enrichment devices which has multipole use in biomedical engineering [3]. Also it has a wide application as electrolyte material for solid oxide fuel cell (SOFC). The most critical parameters for these applications is the dense microstructure, mechanical properties and the ionic conductivity. These properties are dependent on various parameters which include the processing technology of the powders, particle sizes and sintered density [4]. Electrical and mechanical properties of YSZ electrolyte can be enhanced by preparing a fully dense ceramic body upon sintering. In order to achieve the same the powder needs to be ultrafine with a narrow size distribution [5]. The conventional solid state reaction method usually produces large particle sizes and inhomogeneity [6]. Using nano crystalline powder, it is possible to reduce the sintering temperature of the same [7]. Thus various process have been developed for production of YSZ nano- powders such as co- precipitation technique [8], sol-gel preparation [9], hydrothermal synthesis [10] etc. However in all these cases, multi-step reaction routes are required and the processes are relatively complex. Gas phase route, such as flame synthesis is having an advantage of producing nanocrystalline particles with better homogeneity and can be easily scaled-up to industrial level. Different phases of stabilized zirconia powders can be obtained by flame synthesis process. It has been observed that tetragonal phase of zirconia can be obtained by atomizing a solution consisting of zirconium sulfate in water or alcohol in presence of natural gas or carbon monoxide and hydrogen flame [11]. Zirconium n butoxide in butanol solution was used to prepare nanopowders of 12 – 21 nm crystallite size by flame synthesis process with tetragonal as major and monoclinic as minor phase [12]. Fully tetragonal phase zirconia nanoparticle was also prepared from n- butoxide solution with a mean crystallite size of 10 nm 90 nm [13]. Using organic solvents monoclinic zirconia nano- particles were produced at a higher production rate of 300 to 1100 g/hr [14]. However it is difficult to handle organic solvents in an industrial scale. Hence the study for possibility of using water as a solvent in place of organic solvent like benzene, propane and ethanol is required to be investigated. Dense and homogeneous particle through flame synthesis can be obtained if the decomposition point of the precursors is lesser than the boiling point of solvent. Nitrate precursors of zirconia, such as zirconyl nitrate and yttrium nitrate has a decomposition temperature lesser than 1000°C. Limited work has been reported on the possibility of direct synthesis of fully stabilized zirconia by such a route using aqueous solvent and to understand the sintering behavior of same. Hence, there is a case for the use of a flame based processing route for the direct synthesis of agglomeration-free, nanocrystalline yttria stabilized cubic zirconia using aqueous solvent and the sintering behavior of the same.

Experimental Procedure

YSZ Powder Preparation

Zirconyl nitrate anhydrate ($ZrO(NO_3)_2$, Molecular Weight: 231.23) and yttrium nitrate hexahydrate ($Y(NO_3)_3.6H_2O$, Molecular Weight: 383.01) were selected as precursors for preparing the solution for Flame Synthesis. The Yttria (Y_2O_3) content was systematically varied at 8 mol% (abbreviated as 8YSZ), 10 mol% (abbreviated as 10YSZ) and 12 mol% (abbreviated as 12YSZ). For all the three batches the overall concentration of the solution was maintained at 1(M). The nitrate precursors were mixed in water by magnetic stirrer at a RPM of 300-400 until a clear solution was obtained.

Flame Synthesis Process

The modular flame reactor set-up used to conduct the experiments and preparation of nanocrystalline powders basically consisted of a precursor delivery system, a multi-port diffusion burner within a reaction chamber, particle collection unit and vacuum generation system. A schematic flow diagram of the same has been shown in figure 1a and the picture of the same has been shown in figure 1b. The mixed precursors were supplied to the burner and reaction chamber by atomizing the same with an ultrasonic nebulizer. Oxygen was used as both carrier gas and combustion gas. LPG was used as fuel for generating the flame. The flow rate of flammable gas (LPG) was maintained at 20 SCC and that of combustion gas and carrier gas was maintained at 20 slm and 5 slm respectively with a suitable mass flow controller (MKS make). Reaction chamber was made of stainless steel and capable of hermetically sealed with glass view port. The reaction chamber was placed vertically and consisted of a multiport co-flow diffusion burner at bottom. A schematic of the diffusion burner is given in figure 2a and an actual photograph of same is presented in figure 2b. The same configuration enabled independent control of the flow rates of each gas. The flame has been established at the burner head by a spark generator which has been

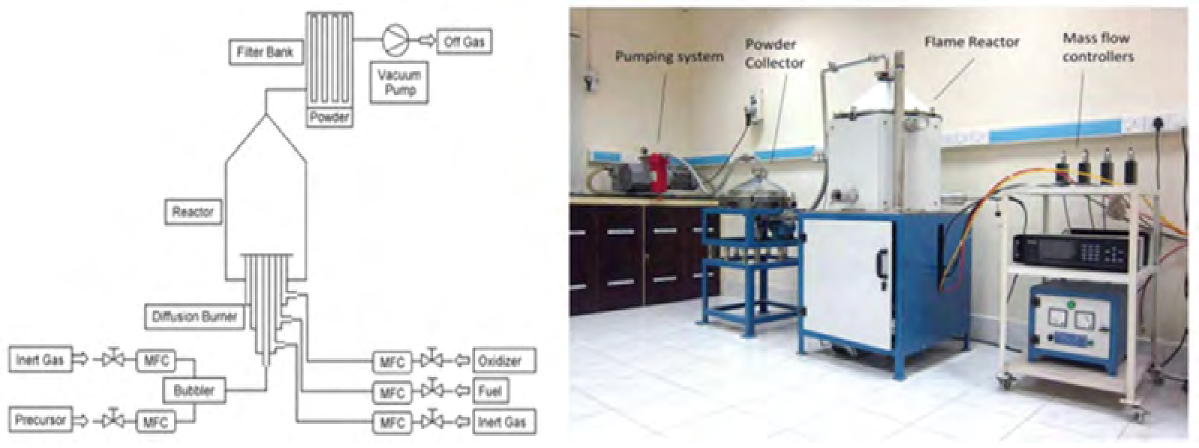

(a) (b)

Figure 1: Schematic (a) and photograph (b) of the experimental set-up used in the flame synthesis of nanocrystalline ZrO_2.

directly placed on the top of the burner and retarded once the flame has been established. The zirconia particles produced from the process were trapped by the filter unit array in the particle collection unit. To maintain a constant flow of gases and reaction products from the reaction chamber to the particle collector unit, a vacuum pump (PVR make, 65 m^3/min capacity) was used. After completion of the experiment, the zirconia nanocrystalline powders were collected from the filter and characterized.

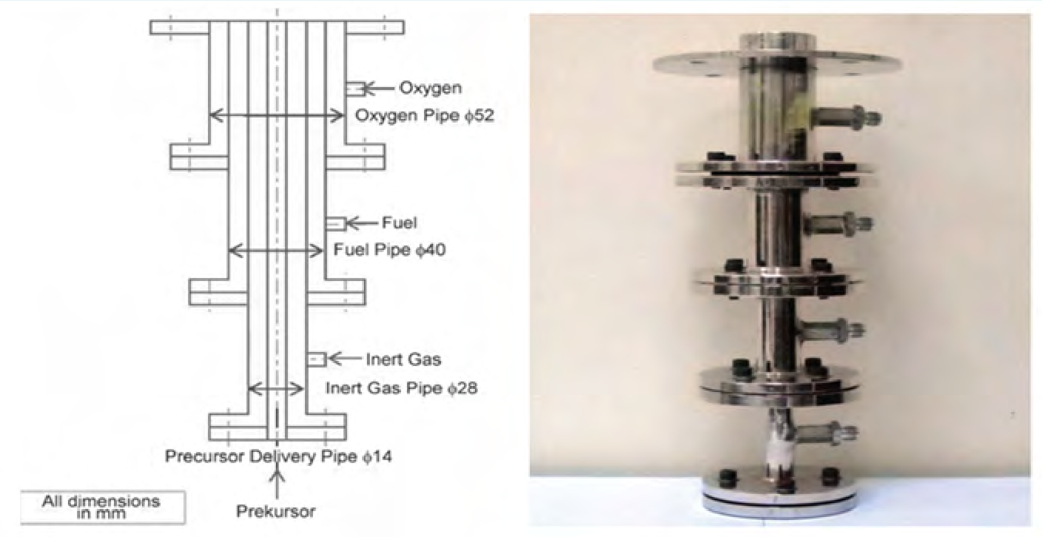

Figure 2: Schematic (a) and photograph (b) of the diffusion burner used in the flame synthesis.

Powder Characterization

The crystallinity and phases were confirmed by X-ray diffraction (XRD) analysis with a PANalytical X' Pert PRO diffractometer using Cu K alpha radiation (λ= 1.5418Å). The crystallite sizes, d_{xrd} of the prepared powders were calculated following Scherrer's equation:

$$d_{xrd} = \frac{0.9\lambda}{\beta \cos\theta} \qquad (1)$$

where λ is the wavelength of the x-ray (0.154 nm) and β and θ represent the measured FWHM and the diffraction angle, respectively.

The specific surface area of the powders were measured by nitrogen absorption following a BET (Brunauer-Emmett-Teller) method using Flowsorb 2300 following ASTM Standard of C 1069-09. Assuming mono-disperse uniform particles, the average effective primary particle size d_{BET} was calculated using the formula,

$$d_{BET} = \frac{6}{S\rho} \qquad (2)$$

where, S is the specific surface area and ρ is the density. Assuming that the crystallites and particles to be nearly spherical in shape, the degree of agglomeration N was found by the equation:

$$N = \frac{d^3{}_{BET}}{d^3{}_{XRD}} \qquad (3)$$

The powder morphology of the prepared nanopowders were analyzed by scanning electron microscopy and transmission electron microscopy. A high resolution scanning electron microscope (FEI Quanta 400F) operating at 20 kv was used to characterize the size and morphology of the prepared nano-crystalline powder. TEM samples were prepared by ultrasonically dispersing the powder in alcohol and subsequently placing it on a carbon coated copper grid. TEM investigations were performed on FEI-Technai T20. Samples for sintering study was prepared by cold pressing of the synthesized nanopowders. Prior to cold pressing, the same was mixed with 0.5% PVA as binder. A sample size of 8 mm diaX10 mm thick was used for sintering study. Sintering study was carried out at a constant rate of heating of 10°C/min up to a temperature of 1650°C. A dwell time of 60 mins have been provided to understand if any changes occurred during this period. The sintering study for the as prepared nanocrystalline powders were performed by Netzsch dilatometer DIL 402E. The change in length with temperature was recorded and the results were analyzed with the help of Netscz proteous software.

Results and Discussions

Powder Characterization

Figure 3 shows the X ray diffraction patterns of YSZ powders synthesized by flame synthesis process. For 10YSZ and 12YSZ powders, fully cubic phase was obtained without any calcination. This is one of the important advantage, since calcination of same will result in increasing crystallite size and grain size. In case of 8YSZ powder, the same was a mixture of tetragonal and cubic phases. The crystallite size of the tetragonal phase was 52 nm while the crystallite size of the cubic phase found to be 56 nm. The average crystallite size of completely cubic phased 10YSZ and 12YSZ powder was found to be 61 nm and 63 nm. The full stabilization was happened with increase in yttria, while an increase in crystallite size was also observed. The average crystallite size (D_{XRD}), specific surface area (S), average particle size (calculated from specific surface area, D_{BET}) and agglomeration ratio N for each sample has been provided in table 1. From the comparable values of d_{BET} and d_{XRD}, it is evident that the synthesized powder was nonagglomerated in nature.

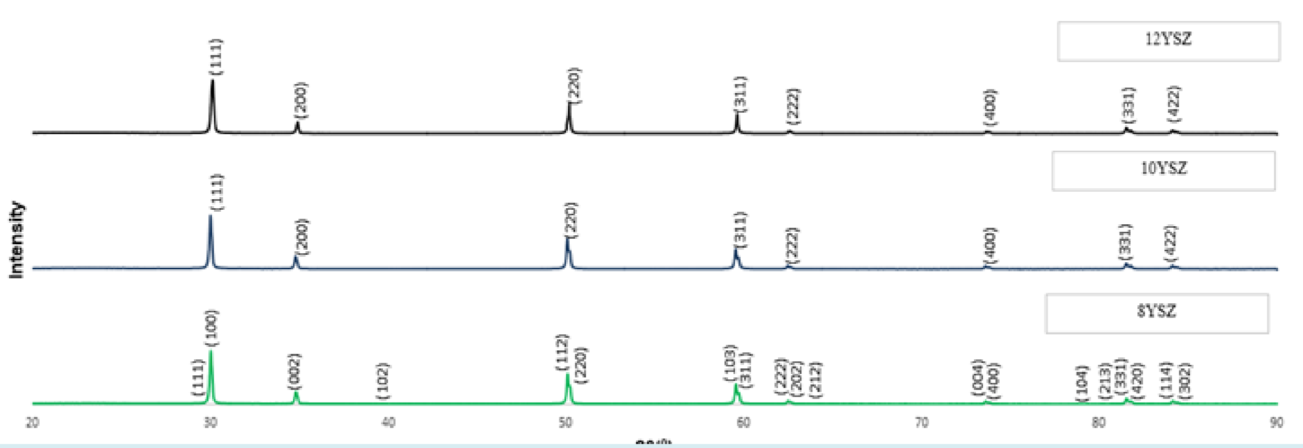

Figure 3: XRD patterns of nanocrystalline ZrO2 with yttria content of 8 mol%, 10 mol% and 12 mol%.

Yttria Content [%]	Specific Surface Area [m^2/g]	d_{BET} [nm]	d_{XRD} [nm]	$N=d^3_{BET}/d^3_{XRD}$
8	15	68	52 for t 56 for c	1.79
10	14	74	61	1.78
12	14.5	71	63	1.43

Table 1: Effect of varying yttria content on particle size and degree of agglomeration in flame synthesis of nanocrystalline zirconia.

The morphology of the as-synthesized ZrO_2 particles was found to be completely spherical in case of all yttria content. The SEM pictures are presented in Figure 4a- 4c in the form. Although a small quantity of agglomerates can be seen, most of the particles are of uniform size. It is well known that temperature, residence time and reaction kinetics affect the particle morphology during flame synthesis. In general, if the rate of sintering is slower than the rate of collision of particles, then agglomerated particles are formed. On the other hand, if the sintering is faster than the rate of collisions, then regularly shaped spherical particles are formed [15-17]. The TEM image reveals that the as synthesized YSZ powder for all the batches are agglomerates of nanoparticles. The size calculated from the TEM images (Figures 5a- 5c) is matching with that of the value obtained by BET method. There seems to be no effect in the morphology of the particles with increasing amount of yttria. From the XRD and TEM study, it was observed that the degree of agglomeration is low in the as synthesized powder. However SEM image shows that there is certain degree of agglomeration, forming a shell type particle structure. Normal distribution graph was prepared from the SEM particle size results and the same was provided in Figures 6a-6c. A mono-modal, fairly narrow particle size distribution has been obtained for all the experiments. Table 2 gives the mean particle size from SEM and TEM study and standard deviations of the powders synthesized with different yttria content.

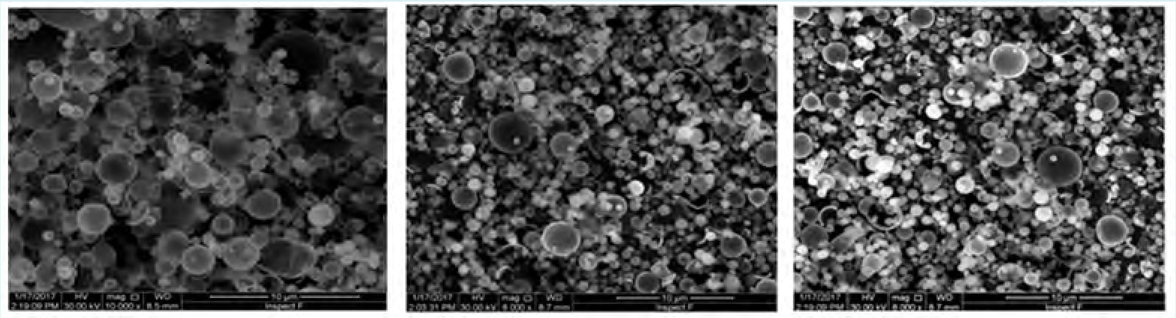

Figure 4: SEM image of as prepared nano-crystalline powder prepared from aqueous precursor solution, (a) 8YSZ, (b) 10 YSZ, (c) 12YSZ.

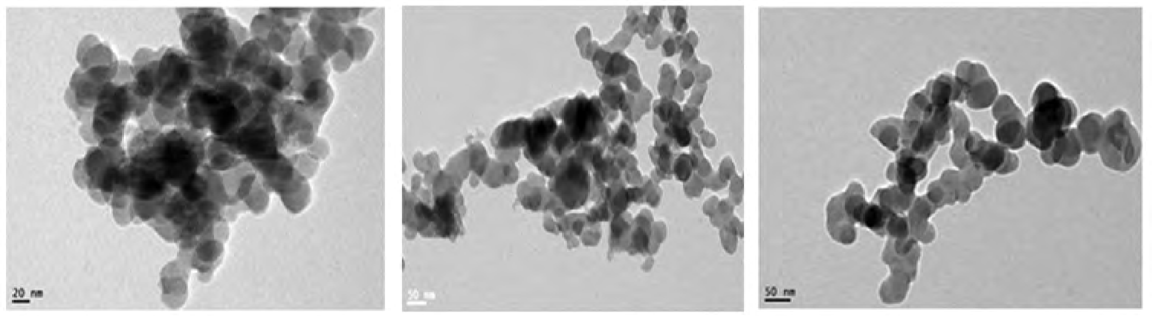

Figure 5: TEM image of as prepared nano-crystalline powder prepared from aqueous precursor solution, (a) 8YSZ, (b) 10 YSZ, (c) 12YSZ.

Yttria Content (%)	Particle Size from SEM (nm)	Primary Particle Size from TEM (nm)
8	122 (28-515)	55 (45-168)
10	142 (57-662)	65 (46-171)
12	146 (56-683)	69 (49-178)

Table 2: Mean particle size from SEM and TEM study and standard deviation of flame synthesized nanocrystalline zirconia.

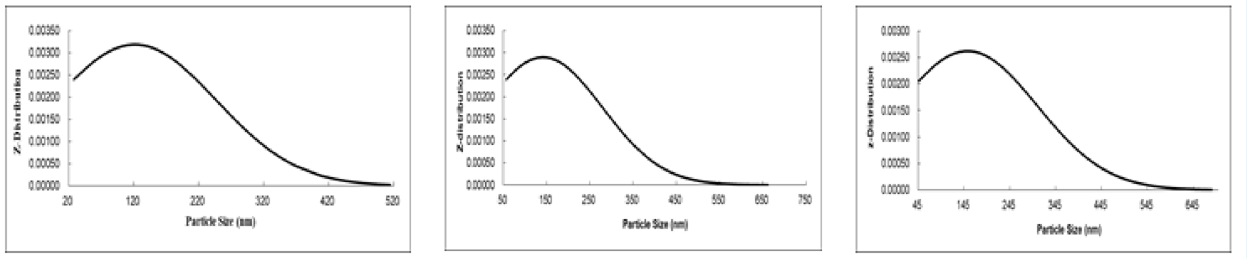

Figure 6: Particle size distribution of nanocrystalline ZrO_2 with various yttria content from SEM study, (a) 8YSZ, (b) 10YSZ, (c) 12YSZ.

Sintering Study

The shrinkage behaviour with temperature for prepared nanopowders are obtained using Netzsch dilatometer with a sample size of 8 mm dia X 10 mm thick. The shrinkage curve was recalculated to the densification curve according to the equation provided below [18]:

$$\rho(t,T) = {(\rho_{g} X100^3)}\Big/{(100+\xi_{(t,T)})^3} \quad (4)$$

where, $\rho(t, T)$= density at the particular temperature and time

ρ_{gd}= green Bulk Density

$\xi_{(t,T)}$ = shrinkage at the particular temperature and time

The sintering curve for all the batches is provided in Figure 7a- 7c. And the densification curve is provided in Figure 8a-8c.

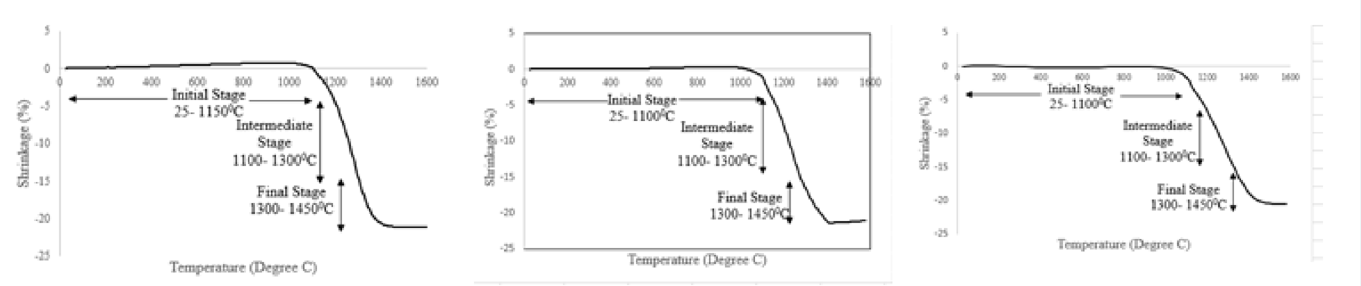

Figure 7: Sintering curve of the as synthesized zirconia nano-crystalline powders, (a) 8YSZ, (b) 10YSZ, (c) 12YSZ.

The activation energy for the densification was calculated from the slope of the densification curve using the formula:

$$\ln\left(T'\frac{d\rho}{dt}\right) = -\frac{Q}{RT} + \ln[f(\rho)] + \ln A \quad (5)$$

Where, T= absolute specimen temperature, T'= heating rate, Q= Activation Energy, $f(\rho)$ = function of density, A= material parameter

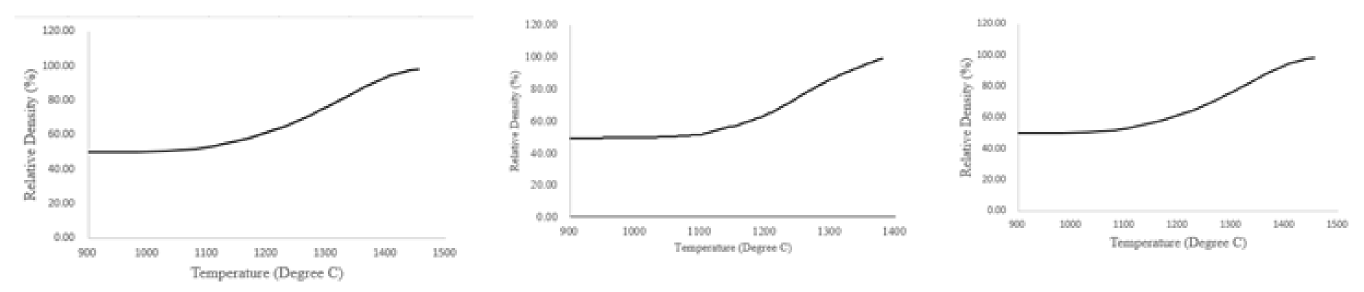

Figure 8: Temperature vs relative density curve of the as synthesized zirconia nano-crystalline powders, (a) 8YSZ, (b) 10YSZ, (c) 12YSZ.

The activation energy for all the three batches, 8YSZ, 10YSZ and 12YSZ are around 210 kJmol^{-1}. The earlier reported values for yttria stabilized zirconia submicron powder was 550 kJmol^{-1} and for nanocrystalline powder was 237 kJmol^{-1} [19-27]. In the latter case, the nanocrystalline yttria stabilized zirconia powder was prepared by a sol-gel process and the primary particle size was 80 nm. The lower activation energy for sintering was due to the finer crystallite size and the nano-sized primary particles. In the present case, the activation energy for the flame synthesized nanopowders is marginally lower and is attributed to even smaller particle and crystallite sizes. It might also due to the high curvature of the surface (because of the smaller sizes) as well as the high specific surface area of the nanopowders, leading to a higher driving force for sintering. Homogeneous distribution led to an improved particle to particle contact and hence, better sintering behavior.

Sl. No	Attributes	Unit	8YSZ	10YSZ	12YSZ
1	Peak temperature	0C	1320	1318	1320
2	Sintering End Temperature	0C	1395	1390	1395
3	Relative Density	%	99.2	99.1	99.09
4	Activation Energy	kJ/ mol	213.5	209.2	209.5

Table 3: Summarized results of dilatometer study for flame synthesized nano- crystalline powder.

More than 99% of true density was achieved for all the batches, which in turn signifies very good sinterability of same. The SEM micrographs are provided in Figures 9a-9c. The microstructure obtained showed dense structure without having any porosity. This type of good microstructure with reduced defect will be helpful in increasing the strength of the material which is also one of the important parameter for designing of thin electrolyte for sensors, membranes for oxygen separators and also for electrolyte for SOFC.

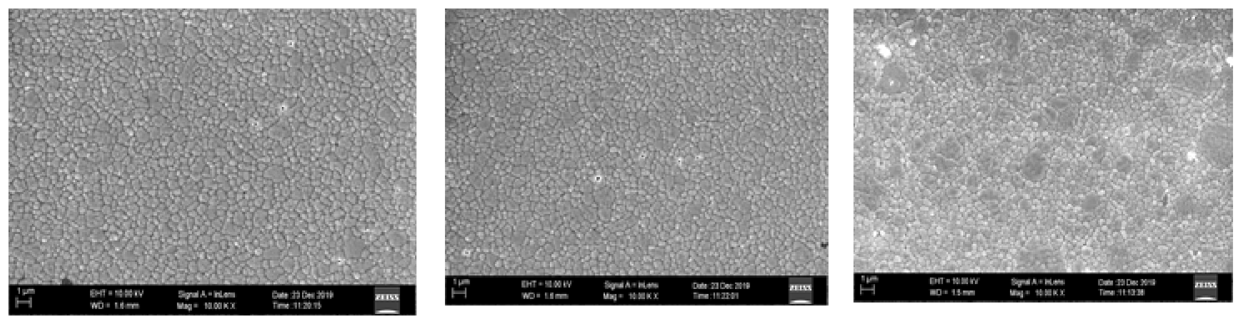

Figure 9: SEM image of the sintered samples prepared from as synthesized zirconia nano-crystalline powders, (a) 8YSZ, (b) 10YSZ, (c) 12YSZ.

Conclusion

A flame synthesis method of synthesizing fully stabilized YSZ nanocrystalline powders was developed in a single step process which does not require any further calcination or any other kind of thermal treatment procedure which in turn will result in increasing crystallite sizes. Synthesis of stabilized nanocrystalline zirconia was successfully carried out by the oxidation and pyrolysis of inorganic aqueous based nitrate precursors. The as synthesized powders exhibited cubic structure without any further calcination step except for 8YSZ where a predominant amount of tetragonal phase was found. The crystallite sizes of the synthesized powders are in nano regime. Specific surface area of the powders are found to be in the range of 14- 15 m^2/ g. The primary particle size was calculated from BET value which indicates that the primary particles are almost free from agglomerates. From the XRD and TEM image study, it is observed that the degree of agglomeration is low in the as synthesized powder. However SEM image shows that there is certain degree of agglomeration, forming a shell type particle structure. It can be concluded that it is possible to prepare nano crystalline fully stabilized zirconia nano powders by flame synthesis process, using inorganic precursors and water as a solvent. The prepared nanopowders are further processed for pressureless sintering. The sintering behaviour of same was studied with dilatometer. The activation energy (210 kJ/mol) of the as prepared nano powders are lower than that of the previous reported value for sub- micron powder (550 kJ/mol) and nano- powder (237 kJ/mol). The highly granular synthesized nanopowders results in high curvature of the surface area, which lower the activation energy of same. Higher sinterability of the same will be helpful to process it for producing further sintered product such as solid state electrolyte for SOFC, oxygen sensor or oxygen pumps. The process for preparing zirconia nano powders using water as a solvent will be helpful for producing the same in high production rate and lower cost and thus the use of organic solvents and regeneration of same can be avoided using water as solvent.

References

1. Fatin Nurwahdah Ahmad, Norazlianie Sazali, Safwan Shalbi, Nor Hasrul Akhmal Ngadiman, Mohd Hafiz Dzarfan Othman (2019) Oxygen Separation Process using Ceramic-Based Membrane: A Review. Journal of Advanced Research in Fluid Mechanics and Thermal Sciences 62(1): 1-9.

2. Chong KC, Lai SO, Thiam HS, Teoh HC, Heng SL (2016) Recent progress of oxygen/nitrogen separation using membrane technology. Journal of Engineering Science and Technology 11(7): 1016-1030.

3. Guanghao Shen, Xiaoming Wu, Chi Tang, Yili Yan, Juan Liu, et al. (2013) An oxygen enrichment device for lowlanders ascending to high altitude. Biomedical Engineering Online 2: 100.

4. Gibson IR, Dransfield GP, Irvine JTS (1998) Sinterability of commercial 8 mol% yttria-stabilized zirconia powders and the effect of sintered density on the ionic conductivity. Journal of Materials Science 33: 4297-4305.

5. Singhal SC, Kendall K (2004) High Temperature Solid Oxide Fuel Cells: Fundamentals, Design and Applications, 2nd (Edn.), Elsevier.

6. He T, He Q, Wang N (2005) Synthesis of nano-sized YSZ powders from glycine-nitrate process and optimization of their properties. Journal of Alloys and Compounds 396(1-2): 309-315.

7. Valefi M, Falamaki C, Ebadzadeh T, Hashjin MS (2007) New insights of the glycine-nitrate process for the synthesis of nanocrystalline 8YSZ. Journal of the American Ceramic Society 90(7): 2008-2014.

8. Keshimiri M, Kesler O (2006) Colloidal formation of monodisperse YSZ spheres: kinetics of nucleation and growth. Acta Materialia 54(16): 4149-4157.

9. Suciu C, Hoffmann AC, Kosinski P (2008) Obtaining YSZ nanoparticles by the sol–gel method with sucrose and pectin as organic precursors. Journal of Materials Processing Technology 202(1-3): 316-320.

10. Dell Agli G, Mascolo G (2004) Zirconia-yttria (8 mol%) powders hydrothermally synthesized from different Y-based precursors. Journal of the European Ceramic Society 24(6): 915-918.

11. Karthikeyan J, Berndt CC, Tikkanen J, Wang JY, King AH (1997) Nanomaterial powders and deposits prepared by flame spray processing of liquid precursors. Nanostruct Mater 8(1): 61-74.

12. Limaye AU, Helble JJ (2002) Morphological Control of Zirconia Nanoparticles through Combustion Aerosol Synthesis. J Am Ceram Soc 85(5): 1127-1132.

13. Roger Muller, Rainer Jossen, Sotiris Pratsinis E (2004) Zirconia Nanoparticles Made in Spray Flames at High Production Rates. J Am Ceramic Society 87(2): 197-202.

14. Jossen R, Mueller R, Pratsinis SE, Watson M, Akhtar MK (2005) Nanotechnology, Morphology and composition of spray-flame-made yttria-stabilized zirconia nanoparticles. Nanotechnology 16(7): 609-617.

15. Ulrich GD, Subramanian NS (1977) Particle growth in flames: Coalescence as a rate controlling process. Combustion Sci Technol 17(4): 119-126.

16. Koch W, Friedlander SK (1990) The effect of particle coalescence on the surface area of a coagulating aerosol. J Colloid Interface Sci 140(2): 419-427.

17. Lehtinen KEJ, Windeler RS, Friedlander SK (1996) Prediction of nanoparticle size and the onset of dendrite formation using the method of characteristic times. J Aerosol Sci 27(6): 883-896.

18. Maca K, Pouchly V, Boccaccini AR (2008) Sintering densification curve: A practical approach for its construction from dilatometric shrinkage data. Science of Sintering 40: 117-122.

19. Maca K, Trunec M, Dobsak P (2005) Bulk Zirconia Nanoceramics Prepared by Cold Isostatic Pressing and Pressureless Sintering. Rev Adv Mater Sci 10: 84-88.

20. Braun JH (1997) Titanium Dioxide-A Review. J Coat Technol 69(868): 59-72.

21. Torabmostaedi H, Zhang T, Foot P, Dembele S, Fernandez C (2013) Process control for the synthesis of ZrO2 nanoparticles using FSP at high production rate. Powder Technology 246: 419-433.

22. Katz JL, Miquel PF (1994) Particle Size and Pore Structure Characterization of Silver Nanoparticles Prepared by Confined Arc Plasma. Nanostructured Mater 4(5): 551-575.

23. Laine RM, Waldner K, Bickmore C, Treadwell DR (1999) Ultrafine metal oxide powders by flame spray pyrolysis. FPO.

24. Sokolowski M, Sokolowska A, Michalski A, Gokieli B (1977) The “In-Flame-Reaction” Method for Al2O3 Aerosol Formation. J Aerosol Sci 8(4): 219-225.

25. Marshall BS, Telford I, Wood R (1971) A field method for the determination of zinc oxide fume in air. Analyst 96(145): 569-578.

26. Qigen Wang, Ranran Peng, Changrong Xia, Wei Zhu, Huanting Wang (2008) Characteristics of YSZ synthesized with a glycine-nitrate process. Ceramics Interational 34: 1773-1778.

27. Strobel R, Pratsinis SE (2007) Flame Aerosol Synthesis of Smart Nanostructured Materials. J Mater Chem 17(45): 4743-4756.